sustainability

MDPI

Article

Environmental, Economical and Technological Analysis of MQL-Assisted Machining of Al-Mg-Zr Alloy Using PCD Tool

Md. Rezaul Karim [1], Juairiya Binte Tariq [1], Shah Murtoza Morshed [1], Sabbir Hossain Shawon [1], Abir Hasan [1], Chander Prakash [2,*], Sunpreet Singh [3], Raman Kumar [4,*], Yadaiah Nirsanametla [5] and Catalin I. Pruncu [6,7,*]

1 Department of Mechanical and Production Engineering, Ahsanullah University of Science and Technology, Dhaka 1208, Bangladesh; rknayeem.mpe@aust.edu (M.R.K.); bintetariq.bd@gmail.com (J.B.T.); shahmurtozamorshed@gmail.com (S.M.M.); sabbirhossain.shawon1@gmail.com (S.H.S.); abirhasan100941@gmail.com (A.H.)
2 School of Mechanical Engineering, Lovely Professional University, Punjab, Phagwara 144411, India
3 Department of Mechanical Engineering, National University of Singapore, Singapore 119077, Singapore; snprt.singh@gmail.com
4 Department of Mechanical Engineering, Guru Nanak Dev Engineering College, Punjab, Ludhiana 141006, India
5 Department of Mechanical Engineering, North Eastern Regional Institute of Science and Technology, Nirjuli 791109, India; yaadudme@gmail.com
6 Department of Mechanical Engineering, Imperial College London, Exhibition Road, London SW7 2AZ, UK
7 Department of Design, Manufacturing & Engineering Management, University of Strathclyde, Glasgow G1 1XJ, Scotland, UK
* Correspondence: chander.mechengg@gmail.com (C.P.); sehgal91@yahoo.co.in (R.K.); catalin.pruncu@strath.ac.uk or c.pruncu@imperial.ac.uk (C.I.P.)

check for updates

Citation: Karim, M.R.; Tariq, J.B.; Morshed, S.M.; Shawon, S.H.; Hasan, A.; Prakash, C.; Singh, S.; Kumar, R.; Nirsanametla, Y.; Pruncu, C.I. Environmental, Economical and Technological Analysis of MQL-Assisted Machining of Al-Mg-Zr Alloy Using PCD Tool. *Sustainability* **2021**, *13*, 7321. https://doi.org/10.3390/su13137321

Academic Editors: Gilberto Santos and Marc A. Rosen

Received: 8 March 2021
Accepted: 21 June 2021
Published: 30 June 2021

Publisher's Note: MDPI stays neutral with regard to jurisdictional claims in published maps and institutional affiliations.

Abstract: Clean technological machining operations can improve traditional methods' environmental, economic, and technical viability, resulting in sustainability, compatibility, and human-centered machining. This, this work focuses on sustainable machining of Al-Mg-Zr alloy with minimum quantity lubricant (MQL)-assisted machining using a polycrystalline diamond (PCD) tool. The effect of various process parameters on the surface roughness and cutting temperature were analyzed. The Taguchi L_{25} orthogonal array-based experimental design has been utilized. Experiments have been carried out in the MQL environment, and pressure was maintained at 8 bar. The multiple responses were optimized using desirability function analysis (DFA). Analysis of variance (ANOVA) shows that cutting speed and depth of cut are the most prominent factors for surface roughness and cutting temperature. Therefore, the DFA suggested that, to attain reasonable response values, a lower to moderate value of depth of cut, cutting speed and feed rate are appreciable. An artificial neural network (ANN) model with four different learning algorithms was used to predict the surface roughness and temperature. Apart from this, to address the sustainability aspect, life cycle assessment (LCA) of MQL-assisted and dry machining has been carried out. Energy consumption, CO_2 emissions, and processing time have been determined for MQL-assisted and dry machining. The results showed that MQL-machining required a very nominal amount of cutting fluid, which produced a smaller carbon footprint. Moreover, very little energy consumption is required in MQL-machining to achieve high material removal and very low tool change.

Keywords: Al-Mg-Zr alloy; minimum quantity lubricant; PCD; optimization; life cycle assessment (LCA); sustainability; energy consumption; CO_2 emission and carbon foot prints

1. Introduction

Alloys have wide applications, such as for use as turbine and furnace components, and in the aerospace and petroleum industries [1]. Aluminum-based alloys have been most widely used in automotive industries due to their excellent formability [2]. There is a

growing trend in Al-based alloy-based metal matrix composites (MMCs) in automotive applications, particularly for engine block manufacturing [3]. The Al/Mg base alloy, combining corrosion resistance with appreciable strength and ductility, is of interest in lightweight structural applications in the transportation industry [4]. Machining of MMC-based composites is challenging compared to conventional steels, so they are often identified as difficult-to-cut materials [5,6]. Some strategies, such as the design of cutting tools, incorporating an appropriate cutting environment, and tool change, are needed to make machining operations more convenient. Sustainable manufacturing is the only solution for developing products via environmentally-friendly, non-polluting, energy-efficient, and economical machining processes to ensure socio-economic wellbeing, safety, and health [7]. According to the Environmental Protection Association (EPA), the use of new cooling/lubrication techniques, such as dry-cutting, MQL, cryogenic cooling, and hybrid cooling techniques in machining, has been acknowledged as a cleaner sustainable machining production approach. Further works from the literature are collected in the following sections.

A number of inserts have been developed to machine hard-to-machine materials. Polycrystalline diamond (PCD) was found to be suitable for machining hardened metals and super-alloys under higher cutting speed conditions [8,9]. To strengthen the efficacy of the PCD tool, an investigation was conducted on Al alloy-based MMC with 20 wt.% of SiC particles, using WC, PCBN, and PCD tools, resulting in PCD providing the best performance as a cutting insert [10]. Furthermore, considering that the hardness of PCD is higher than that of SiC, the efficiency of different tool materials was analyzed while machining Al-based SiC alloy and it was concluded that PCD was superior to the PCBN tool, a coated ceramic tool, and cemented carbide instruments [11].

The PCD inserts with particle SiC and B4C-reinforced MMCs have also been examined for short fibrous Al2O3. Based on the wear rates and morphology of worn surfaces, abrasion by dislodged diamond grains and microcracking caused the wear of PCD. [12]. PCD and chemical vapor deposition (CVD) diamond-coated tools were investigated for tool life, and the initial flank wear on both the tools was generated by abrasion [13]. Chip–tool interface temperature is another important parameter associated with many machining operations. Inherently, high steel production machining offers a high temperature in the cutting area, which leads to substantial deviations and premature failure of cutting tools [14]. High cuts that negatively influence the lifespan of the tool, dimensional precision, and product surface integrity unavoidably characterize high-speed workmanship. However, a high-pressure oil jet can lower the cutting temperature and extend the lifetime of tools to the same extent as the chip–tool interface [15,16].

Rabiei [17] focused on the importance of cutting fluids to facilitate certain benefits during machining, such as improved tool life and a good surface finish. In some applications, between dry machining and flood cooling, an ideal lubrication solution can be found in the form of MQL, which is a viable solution to address the drawbacks of dry and flood-cooling processes [18,19]. Abhang and Hameedullah investigated the effectiveness of the MQL technique depending on the level of the process parameters and the work material, resulting in a reduction of chip-tool interface temperature as high as 30% compared to conventional cooling [20]. The studied effect of MQL on surface roughness in CNC turning determined that a minimal quantity of lubrication could significantly reduce the resultant output when compared with the traditional flood-cooling method [21]. Karim et al. investigated the effect of MQL in turning Al alloy composite using the Taguchi–PCA approach and determined the issue of the beneficial impact of MQL over the conventional cooling method [22,23]. MQL integrated into the turning of AISI 4140 steel could improve the cutting temperature and surface integrity. Adding special additives to the coolant and lubricant systems may also enhance the base fluid's tribological properties by minimizing machining forces and decreasing chip–tool interface temperature [24,25].

While focusing on improving tool life, cutting force, and surface roughness, Lin explored the use of Taguchi analysis during the turning of S45C steel bar using P20 tungsten

carbide. They found that the Taguchi method was a multiple performance optimization solver [26]. In an attempt to predict response parameters, Temel et al. [27] concluded that ANN is an effective method for predicting output variable with a minimum error for identifying mechanical and physical characteristics of Al_20_{24}-B_4C MMC. Bachy and Franke [28] used ANN and RSM to develop laser process mathematical models, and resulted in generating the lowest errors using an artificial neural network, which justified ANN's high precision response concerning surface methodology. Various researcher reported the use of artificial intelligence in the processing of Al-alloys [29–31]. Reddy compared RSM and ANFIS predicted surface roughness values, and the ANFIS results were superior to those of RSM [32]. A fuzzy model was developed using three different sets of process parameters and it was concluded that the ANFIS-based hybrid model was best suited to accurately predict surface roughness, with a MAPE value of 0.113542% compared to the developed ANN model [33].

Energy consumption evaluation is an integral part of life cycle assessment (LCA) and sustainability. Energy consumption varies with the machining stages and depends on the utilization of instruments assisting the machining [34,35]. The utilization of cooling and lubrication systems raised the power produced by the machine [36]. However, an analysis of electric energy usage is not sufficient to determine the sustainability of the machining process. Therefore, consumed resources' incarnated energy has been introduced into research in recent years [37,38]. Carbon (CO_2) emission and carbon footprint analysis is also a key indicator of LCA and sustainability. Ic et al. [39] optimized the processing parameters of a machine to turn Al-7075 alloy to minimize the emission of CO_2 and to produce a low surface roughness. It was reported that the proper selection of coolant reduced the generation of CO_2 emissions and was better for the environment. CO_2 emissions have been found to be approximately zero in the MQL and cryogenically assisted machining process. Production costs are also essential for LCA and sustainability. The production costs of machined components were computed using Taylor's cost method. The model comprised tool cost, machine cost, and tool change cost, but this model does not include a coolant effect on the production costs [40]. Jamil et al. proposed a cost model for dry, MQL, and LN_2-assisted cooling of machining of Ti-alloy, and it was found that the production cost was reduced significantly [41].

The necessity for environmentally friendly machining has always been the motivating factor regarding cutting-fluid-usage reduction techniques. MQL is amongst the most promising machining strategies, allowing for a 90% reduction in cutting fluid consumption, although it also preserves surface quality and tool life. The prominence of MQL in machining necessitates an analysis of MQL progress. During machining operations, flood cooling is a popular method for extracting heat from the cutting field; however, it has negative consequences, such as it can cause respiratory illnesses among employees, environmental issues, and cutting fluid processing and disposal. As a result, environmentally sustainable lubrication solutions must be implemented to address flood lubrication issues. The MQL strategy can also help with machining issues like chip pressure welding to the cutting edge, which is the main reason for tool failure. Additionally, MQL improves the surface quality of machined parts. However, MQL is mainly concerned with reducing friction, rather than removing as much heat as possible by regulating heat generation at its source.

A detailed literature survey has revealed that there is a complete dearth of literature on life cycle assessment (LCA) and sustainability analyses of MQL-assisted machining of Al-Mg-Zr alloy. The sustainability aspect of the machining area requires a great deal of attention and needs to be comprehended in a structured manner in comparative studies. Unfortunately, most academics and manufacturing industries are still focused only on traditional methods. However, insincere efforts have been made in understanding the effects of environmental, economic, and technological analyses of MQL-assisted machining of Al-Mg-Zr Alloy. The present study has created another endeavor, to fill the gap due to the already-stated theoretical research gaps. The current research on MQL-assisted machining of Al-Mg-Zr alloy using a PCD tool has created the following objectives:

- To determine the influence of cutting parameters on sustainable responses, viz. surface roughness and cutting temperature using ANOVA and the main effect of plots using the PCD tool;
- To achieve optimal cutting parameters with the Taguchi method and multi-objective optimization with desirability function analysis (DFA);
- To model cutting parameters with ANN and ANFIS;
- To analyze life cycle and sustainability aspects of MQL-assisted machining of Al-Mg-Zr alloy.

To understand the extent of sustainability analysis on MQL-assisted machining of Al-Mg-Zr alloy, the present study was based on a fundamental analysis of three research questions:

Q1: Do cutting parameters significantly affect sustainable responses or not?
Q2: Do the cutting parameters differ from optimal settings?
Q3: Does a statistically significant interrelationship between parameters contribute to "sustainable machining"?

The rest of the paper is organized as follows: Section 2 details the materials and methods utilized for modeling and optimization, workpiece material, equipment and the instruments used as well as the design of the experiments. Section 3 describes the analysis of results using ANOVA, optimization with the Taguchi method, and multi-objective optimization with DFA, ANN, and ANFIS modeling. Section 4 displays a comparative analysis, including ANN and ANFIS results and life cycle and sustainability analysis, followed by conclusions, limitations, and the future scope of research, in Section 5.

2. Materials and Methods

2.1. Workpiece Material and Dimensions

Aluminum, magnesium, and zirconium were used in this work. A stir casting process with an RPM of 600 was used to prepare the alloy. EDX analysis was carried out to obtain the developed alloy composition, as shown in Table 1 and Figure 1. A cylindrical-shaped alloy was prepared for turning operations, with a length of 305 mm and a diameter of 70 mm.

Table 1. Composition of the developed Al/Mg/Zr alloy.

Element	Weight %	Atomic %
Mg	34.81	51.67
O	11.34	12.63
Al	52.18	34.47
Zr	1.67	1.22

2.2. Cutting Inserts

An SNMG 120408 polycrystalline diamond (PCD) cutting insert with a nose radius of 0.8 mm under minimum quantity lubricant (MQL) cutting conditions was used in the turning process using a center lathe.

2.3. Equipment and Instruments

The roughness was measured using an optical surface profilometer. Each measurement was repeated three time to reduce the error and the mean arithmetic average value was collected.

During the experiments, a thermocouple was used to monitor the cutting temperature. In addition, a digital multi-meter was used to record the electromotive force (emf) in millivolts, with one end of the multi-meter attached to the workpiece and the other end to the tool. The thermocouple calibration maintained the temperature measuring accuracy using comparison techniques. The calibration procedure was achieved according to the ASTM E220 standard test method by trained lab technicians [42].

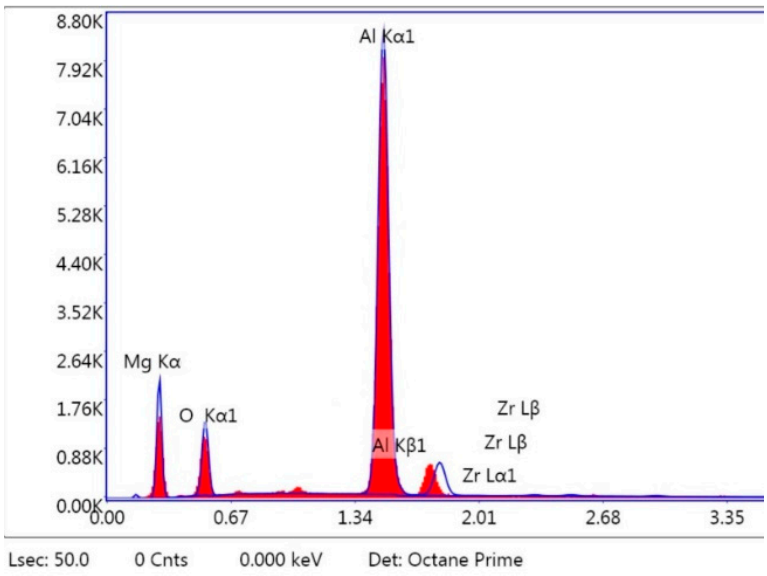

Figure 1. EDX analysis of the Al-Mg-Zr alloy.

2.4. Experimental Setup and Design of Experimentation

Experiments were performed according to Taguchi's methodology [43]. The cutting parameters, such as cutting speed (V_c), feed rate (S_0), and cutting depth (t), using five different levels, were considered. The experiments were conducted to decide the cutting parameter levels along with the tool manufacturing suggestions and the machine tool capacity using an L-25 OA array. The optimization was performed using desirability function analysis, as reported in previous research [44]. The cutting parameters and the allocation of the different levels are shown in Table 1. The standard L_{25} OA as per the cutting parameters levels is shown in Table 2. Each experiment was repeated three times as designed, and the average values of the responses for surface roughness (R_a) and cutting temperature cutting (θ) are shown in Table 3. Figure 2 presents the experimental setup and the method used for the study. The pressure was kept at 8 bar, and the flow rate during machining was kept constant at 120 mL/h.

2.5. ANFIS and ANN Based Predictive Modelling

The adaptive fuzzy inference system (ANFIS)-based network is a hybrid architecture comprising neural and fuzzy logic systems. An information-based technique is used in a neural network stage to provide function-approximation problems [33]. First, a fuzzy inference method with an initial fuzzy model is established, taking into account the fuzzy rules extracted from the input–output data. Then, the neural network is used to fine-tune the built-up original fuzzy model's rules in the next step.

A Sugeno (output is linear or constant) type ANFIS model is used in the present work. The experiment takes three input parameters (depth of cut, cutting speed, and feed rate) and two output parameters (surface roughness and cutting temperature) into consideration. The ANFIS model is constructed using a Gaussian membership function (Gaussmf) with three membership functions for all input parameters and a linear membership function for the output parameter. The hybrid approach is used to maximize parameter performance.

ANN is a common prediction tool that helps to calculate various outputs from different parameters. ANN has three interconnected layers, and core features of the artificial neural network are its learning ability and the various learning algorithms [33]. To get a minimal variance between the experimental values and the output values, it is essential to decide the best learning algorithm and the optimum number of neurons.

Table 2. Experimental input parameters and resultant responses.

	Variable 1	Variable 2	Variable 3	Response 1	Response 2
Run	**t: Depth of Cut (mm)**	**V_c: Cutting Speed (m/min)**	**S_0: Feed Rate (mm/rev.)**	**R_a: Surface Roughness (μm)**	**θ: Cutting Temperature (°C)**
1	0.25	86	0.1	0.508	135.79
2	0.25	112	0.12	0.625	152.24
3	0.25	138	0.14	0.784	173.45
4	0.25	143	0.16	0.815	177.53
5	0.25	178	0.18	1.030	206.09
6	0.45	86	0.12	0.49	134.66
7	0.45	112	0.14	0.735	165.50
8	0.45	138	0.16	0.894	186.77
9	0.45	143	0.18	0.925	190.85
10	0.45	178	0.1	1.140	219.41
11	0.65	86	0.14	0.728	162.43
12	0.65	112	0.16	0.845	178.88
13	0.65	138	0.18	1.004	200.09
14	0.65	143	0.1	1.035	204.17
15	0.65	178	0.12	1.250	232.73
16	0.85	86	0.16	0.795	170.98
17	0.85	112	0.18	0.955	192.20
18	0.85	138	0.1	1.114	213.41
19	0.85	143	0.12	1.145	217.49
20	0.85	178	0.14	1.360	246.05
21	1.25	86	0.18	1.015	197.62
22	1.25	112	0.1	1.175	218.84
23	1.25	138	0.12	1.334	240.05
24	1.25	143	0.14	1.365	244.13
25	1.25	178	0.16	1.580	272.69

Table 3. Cutting parameters and different levels.

Variables	Units	Level 1	Level 2	Level 3	Level 4	Level 5
Depth of cut (t)	mm	0.25	0.45	0.65	0.85	1.25
Cutting speed (Vc)	m/min	86	112	138	143	178
Feed rate (S0)	mm/rev.	0.1	0.12	0.14	0.16	0.18

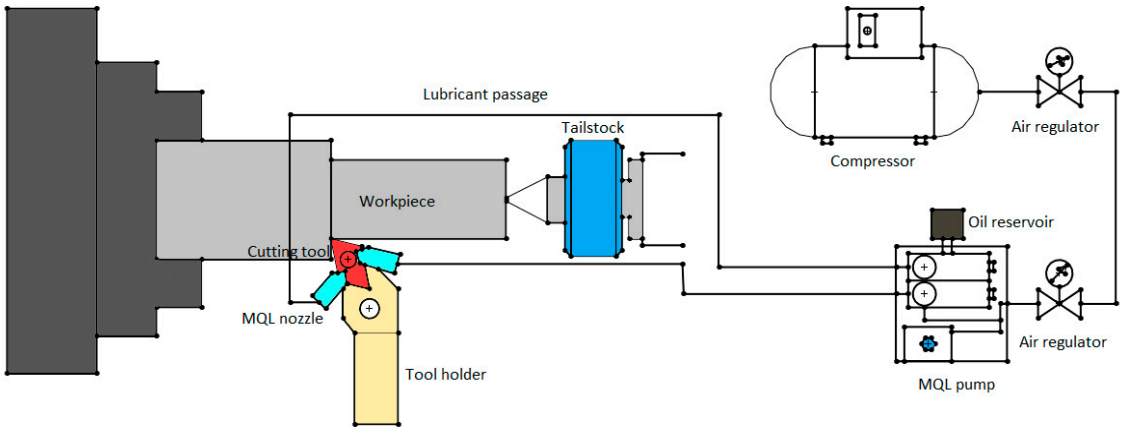

Figure 2. Experimental setup under MQL conditions.

2.6. Data Collection for Sustainability Analysis

PPC-3 power meter load controls were utilized to calculate energy consumption during different phases of machine tooling. In order to obtain the electrical energy consumption in various process stages (functional states of the machine tool), the estimated power was compounded by a known time frame. In the measurement of the lubrication capacity, a smart meter was used. The intelligent meter consisted of Raspberry Pi-3 and a Smart-Pi, keyboard and mouse, an HDMI adapter and a micro SD card. In addition, the proposed uniform approach calculates carbon emissions, as reported in a previous study [45].

3. Results and Discussion

3.1. Effect of Process Paramters on Surface Roughness and Cutting Temprature

An SN ratio shows the influence of each input variable parameter on each regulated parameter level, and the parameter has an impact on the surface roughness and cutting temperature. Since a higher SN is closer to a higher quality, a bigger SN ratio is better. Both Tables 4 and 5 demonstrate that cuts at speeds ranked 1, followed by cutting depth rank 2, had the least impact on the results and the feed rate, as the cutting parameter affected the surface roughness most effectively and the cuts in the temperature quality were in accordance with the SN ratio.

Table 4. Response table for SN ratios (surface roughness).

Level	Depth of Cut	Cutting Speed	Feed Rate
1	0.7528	0.7074	0.9948
2	0.8372	0.8671	0.9692
3	0.9728	1.0268	0.9948
4	1.0743	1.0575	0.9863
5	1.2943	1.2724	0.9863
Delta	0.5415	0.5650	0.0256
Rank	2	1	3

Note: Smaller is better.

Table 5. Response table for SN ratios (cutting temperature).

Level	Depth of Cut	Cutting Speed	Feed Rate
1	−44.47	−44.01	−45.81
2	−44.97	−45.11	−45.59
3	−45.77	−46.09	−45.79
4	−46.30	−46.26	−45.77
5	−47.36	−47.40	−45.90
Delta	2.89	3.39	0.32
Rank	2	1	3

Note: Smaller is better.

Figures 3–6 correspondingly show the principal effect parts for the mean and SN ratios of surface roughness and cutting temperature. It is usually preferable to increase the value of the SN ratio; hence, the ideal cutting conditions can be attained when the SN ratios are highest in all three entry parameters. The primary SN ratio effect plot (Figures 3 and 5) shows that a low roughness and cutting temperature reached at a 0.25-mm cutting depth, 86-m/min cutting speed and a feed-rate of 0.12 mm/rev. Figures 4 and 6 show that the ideal value at a cut-through depth of 0.25 mm, 86 m/min cutting speed and 0.12 mm/rev feed rate was seen for reduced surface roughness and cutting temperature. In order to get the optimum assessment of both surface roughness and cutting temperature, it was proposed that a lower cutting depth, lower cutting speed and low-to-moderate feed rate need to be used.

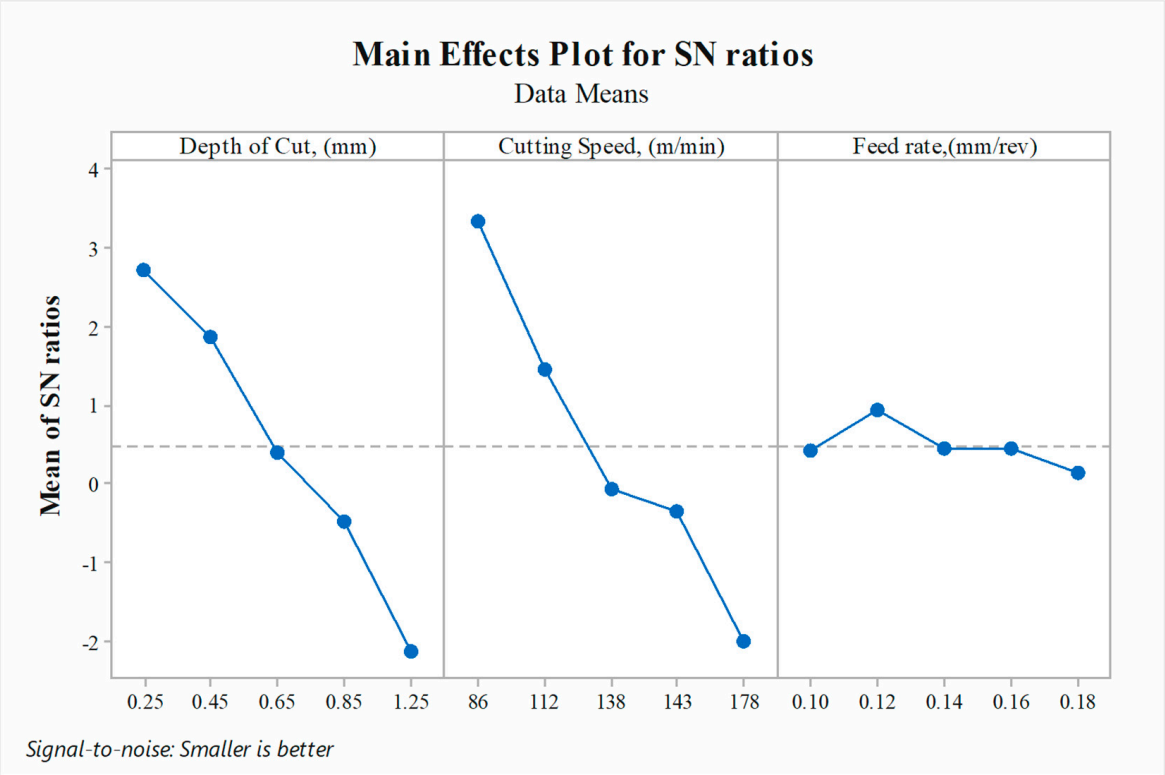

Figure 3. Main effect plots for SN ratios of surface roughness.

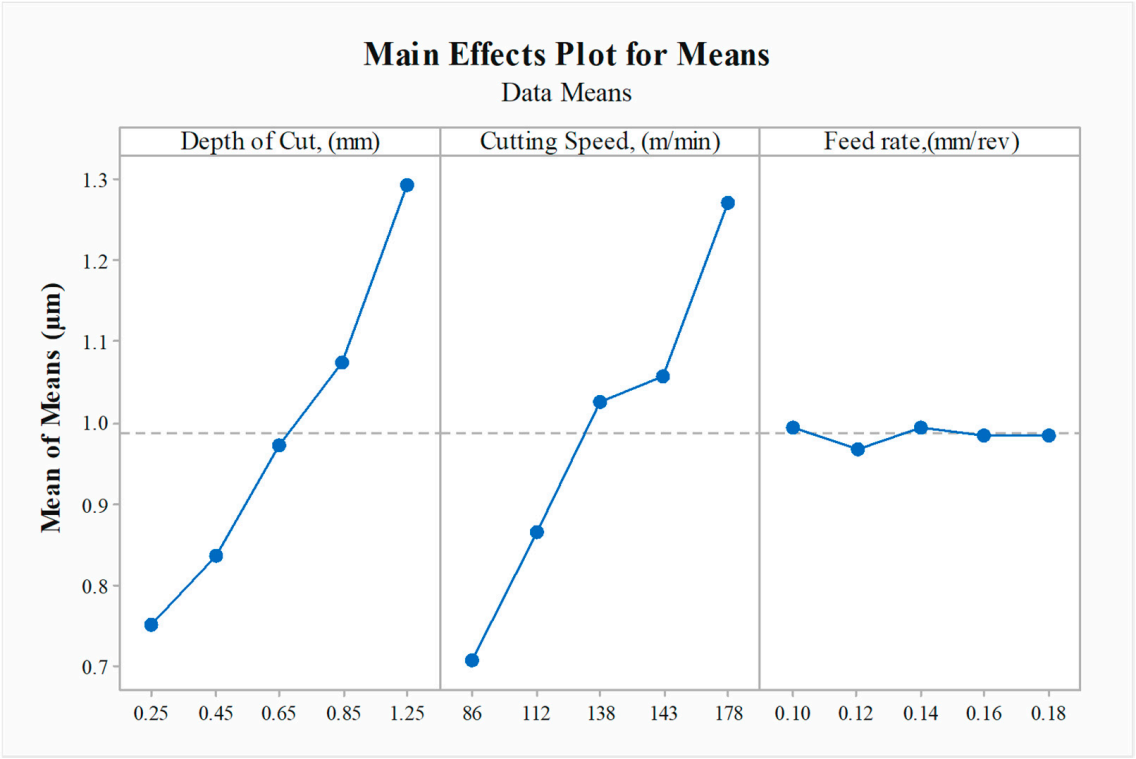

Figure 4. Main effect plots for surface roughness.

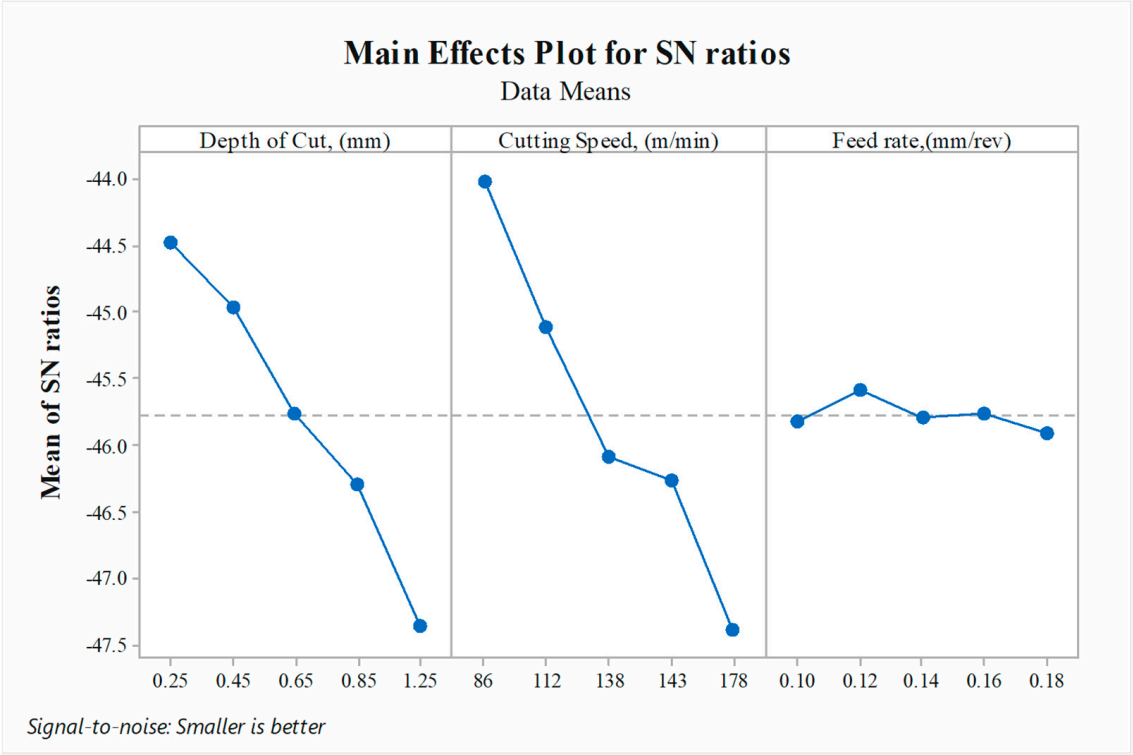

Figure 5. Main effect plots for SN ratios of cutting temperature.

Figure 6. Main effects plot for cutting temperature.

3.2. Analysis of Variance (ANOVA)

In this study, ANOVA was performed for the response of surface roughness and cutting temperature. The sum of the squares (SS), the degrees of freedom (df), the mean square (MS), the *F*-value, and the *p*-value for all input variables are shown in Tables 6 and 7 for the MQL-aided cutting conditions. *p*-values below 0.05 indicate that the terms of the model are noteworthy for both responses. Moreover, it is easily understood from the analyses that the cutting speed and the depth of the cut are the most prominent factors, which is aligned with the results of the S/N ratio analysis. Thus, both the method factors can give an assertion about selecting the dominant factor affecting the process.

Table 6. Analysis of variance for surface roughness.

Source	SS	df	MS	F-Value	*p*-Value	Contribution
Model	1.80	3	0.5995	1152.52	<0.0001	significant
t	0.8956	1	0.8956	1721.90	<0.0001	49.48%
V_c	0.9028	1	0.9028	1735.65	<0.0001	49.87%
S_0	7.688×10^{-9}	1	7.688×10^{-9}	0.0000	0.9970	
Residual	0.0109	21	0.0005			
Cor. Total	1.81	24				

Table 7. Analysis of variance for cutting temperature.

Source	SS	df	MS	F-value	*p*-Value	Contribution
Model	29,087.40	3	9695.80	1462.35	<0.0001	significant
t	13,136.15	1	13,136.15	1981.23	<0.0001	44.94%
V_c	15,951.25	1	15,951.25	2405.82	<0.0001	54.57%
S_0	0.0005	1	0.0005	0.0001	0.9932	
Residual	139.24	21	6.63			
Cor. Total	29,226.64	24				

3.3. Optimization Using Desirability Function Analysis (DFA)

Multi-response optimization aims to determine the independent variable conditions that lead to optimal or nearly optimal values for the response variables. In this desirability function analysis, minimizing surface roughness and cutting force was the prime objective. Factor ranges defined for the basic optimization are shown in Table 8. A summary of the optimization to fulfil the essential purpose of minimizing the response parameter is demonstrated in Table 9 and Figure 7.

Table 8. Goals and factor range for optimization of surface roughness and cutting temperature.

Factor	Goal	Limit		Weight		Importance
		Low	High	Low	High	
t	is in range	0.25	1.25	1	1	3
V_c	minimize	86	178	1	1	3
S_0	is in range	0.1	0.18	1	1	3
R_a	minimize	0.49	1.58042	1	1	4
θ	is in range	134.66	272.698	1	1	4

Table 9. Summary of the values obtained from optimization.

No.	t	V_c	S_0	R_a	θ	Desirability	
1	0.305	86.000	0.180	0.496	134.660	0.997	Selected
2	0.264	89.307	0.180	0.494	134.660	0.983	
3	0.396	86.000	0.180	0.546	140.719	0.970	
4	0.414	86.000	0.180	0.555	141.906	0.965	
5	0.445	86.000	0.100	0.573	143.992	0.956	
6	0.504	86.596	0.100	0.609	148.422	0.933	
7	0.573	89.931	0.100	0.667	155.706	0.887	

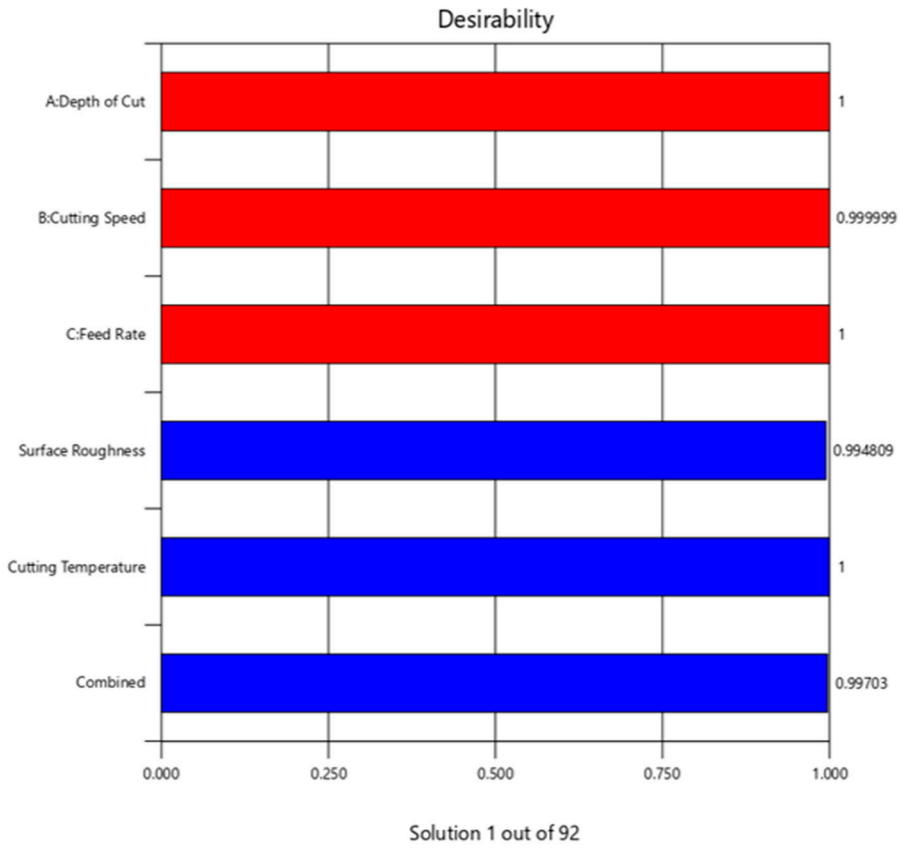

Figure 7. Desirability bar chart for optimum solution.

3.4. Proposed ANN Model

Various learning algorithms, such as LM, CGP, SCG and BFG, are used to determine the most appropriate learning algorithm for predicting surface roughness and cutting temperature. The number of hidden layers were modified to 9, 12, 15, and 20 to achieve the best possible proximity to the experimental results. For an increasing number of hidden layers, the response parameter values were calculated using the correlation coefficient (R^2) comprising all four types of learning algorithms. Of all the algorithms, the LM algorithm was best suited for the training data of the surface roughness and cutting temperature. At the same time, SCG was the most suitable algorithm for testing data collection. When testing with cutting temperature experimental data collection, barring the best network structure for checking the cutting temperature data, i.e., 3-15-2, the best network structure for the remainder of the data set was 3-9-2, as shown in Figure 8. The proposed ANN structure showed that it has three neurons (depth of cut, cutting speed, and feed rate) in the input layer, nine neurons in the hidden layer, and two neurons in the output layer (surface roughness and cutting temperature). In Table 10, the statistical values of the learning algorithm responses are given.

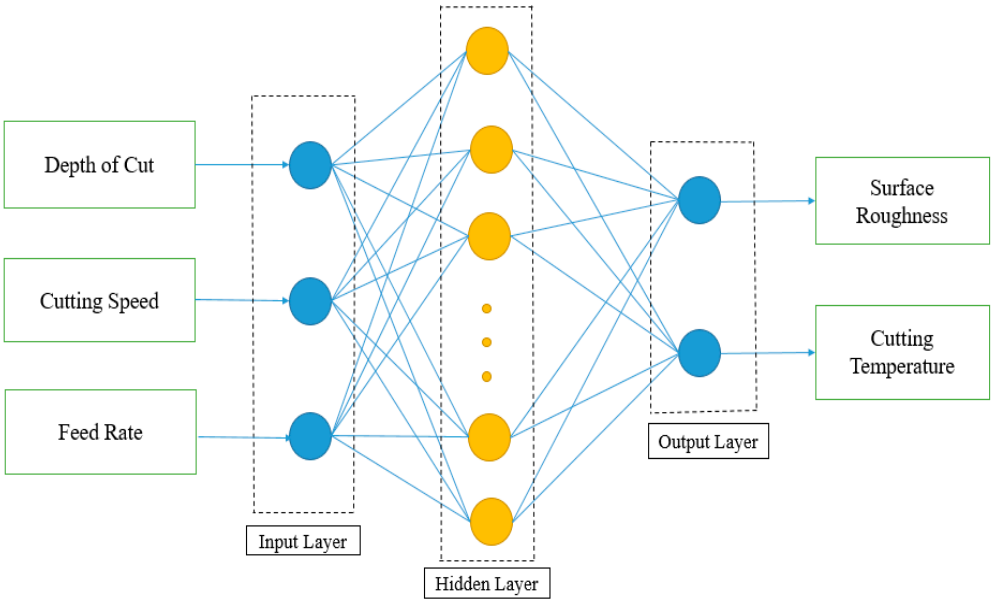

Figure 8. Proposed ANN architecture (3-9-2).

Table 10. Statistical data of the response parameters using different learning algorithms.

Learning Algorithm	No. of Neurons	Training Data		Testing Data	
		R^2		R^2	
		R_a	θ	R_a	θ
LM	9	0.99732	0.99847	0.99643	0.9964
LM	12	0.99612	0.99727	0.9915	0.9927
LM	15	0.99103	0.99218	0.9574	0.9584
LM	20	0.98431	0.98546	0.96487	0.96597
LM	24	0.96356	0.96471	0.97672	0.97773
CGP	9	0.99242	0.99357	0.9943	0.9973
CGP	12	0.99185	0.9928	0.9915	0.9927
CGP	15	0.99151	0.99266	0.99388	0.9948
CGP	20	0.99136	0.99251	0.99467	0.9956
CGP	24	0.99145	0.99260	0.99521	0.9964
SCG	9	0.99137	0.99252	0.99488	0.9974
SCG	12	0.99156	0.99271	0.9944	0.9967
SCG	15	0.99199	0.9929	0.99464	0.9976
SCG	20	0.99161	0.99271	0.99352	0.9975
SCG	24	0.99182	0.99286	0.99351	0.99658
BFG	9	0.99208	0.99328	0.99638	0.9973
BFG	12	0.99215	0.99415	0.99631	0.9971
BFG	15	0.99187	0.99297	0.99563	0.9966
BFG	20	0.99171	0.99276	0.99532	0.9962
BFG	24	0.99181	0.9928	0.99373	0.9947

In this study, 25 experimental data points were arranged for training and testing purposes. Thus, 72% of the data was used for training purposes, while 28% of the data was used for testing purposes; 18 datasets were used for training, and the remaining 7 datasets were used for testing.

3.5. ANFIS Based Predictive Modeling

The hybrid technique is used to examine the test dataset by loading it from the workspace into ANFIS. For all input parameters and linear type membership functions

for output membership functions, FIS was formed using the Gaussian mission function Gaussmf and was shown in Figure 9. The hybrid technique was chosen as the 0 percent error tolerance and 100 epoch optimization approach was used until there was a minimum error in a correct result. Membership function and rules generated by FIS for both the outputs are shown in Figures 10 and 11. The corresponding errors obtained for the surface roughness and the cutting temperature in the hybrid method were 1.107% and 1.172%, respectively, using the rule viewer, as shown in Figure 11. With this changing of the inputs, the resultant output values for the developed hybrid-type ANFIS model was generated.

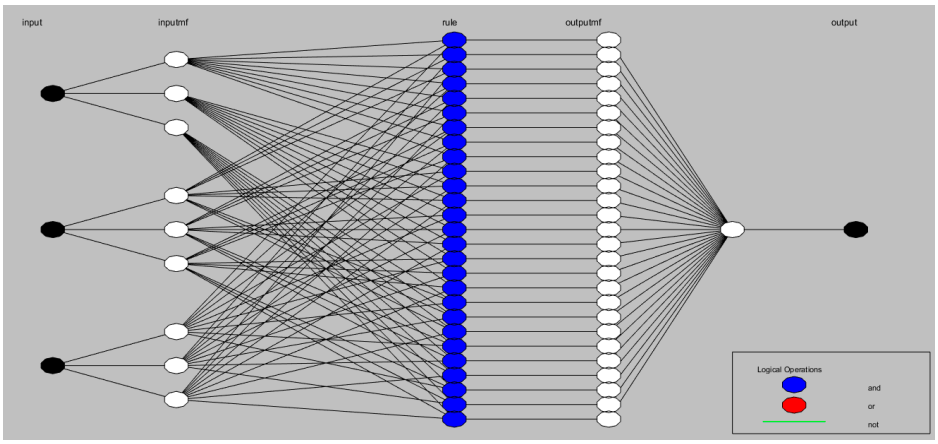

Figure 9. Sugeno ANFIS-based predictive model.

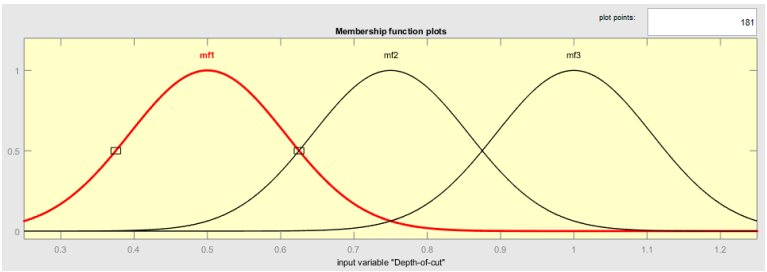

(**a**)

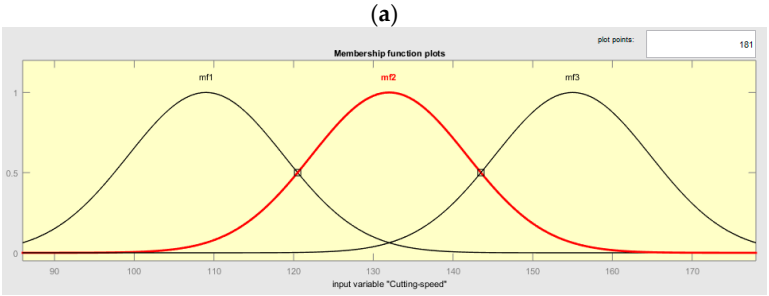

(**b**)

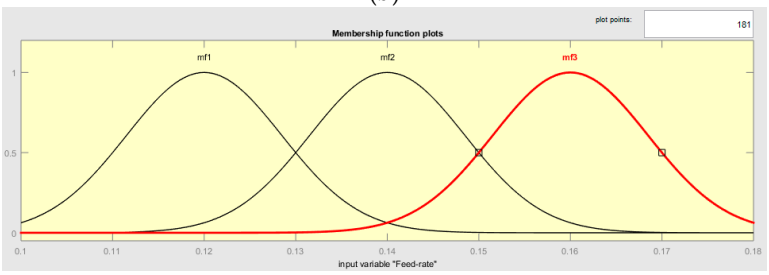

(**c**)

Figure 10. Membership function for input variable (**a**) depth of cut, (**b**) cutting speed, and (**c**) feed rate.

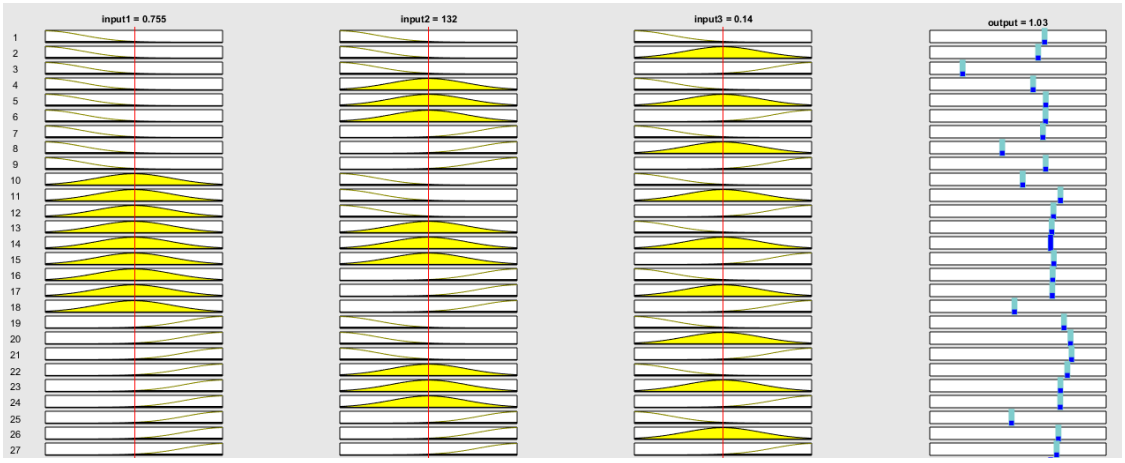

(**a**)

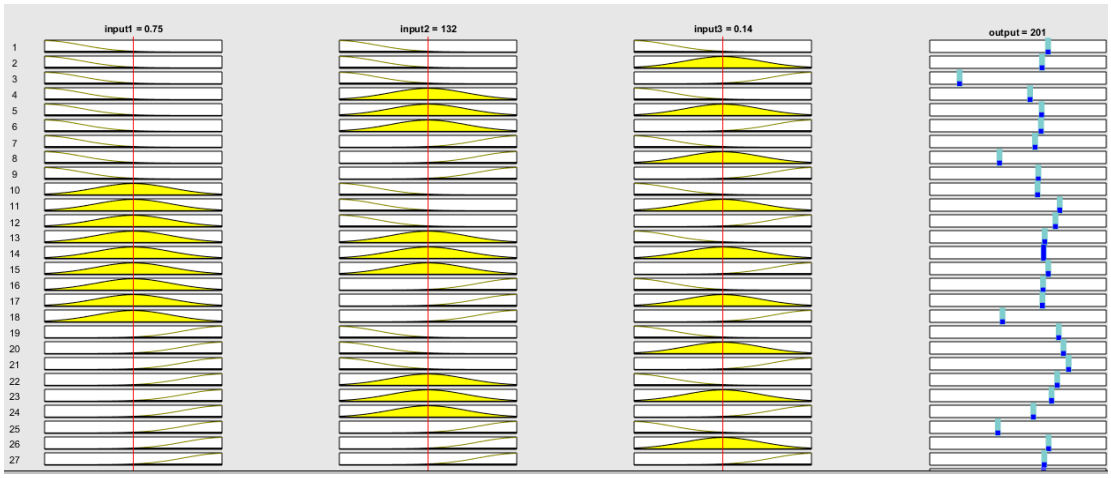

(**b**)

Figure 11. ANFIS-generated rule viewer for (**a**) surface roughness and (**b**) cutting temperature.

3.6. Three-Dimensional Surface Plots

To understand the interaction effects of the input variables on the response factor, 3D surface plots were plotted based on a developed ANFIS-based model, as portrayed in Figure 12. From the surface views, it was found that a three-dimensional curve represented the mapping from any of the two input parameters to the output parameter. The *Z*-axis represents surface roughness and the cutting temperature, while the *X* and *Y* axes represent two input parameters. All the input parameters could be changed to see how they affected the output parameter. The surface plot displays the effect of the feed rate on R_a and θ is negligible compared to the impact of the cutting speed and the depth of cut. This demonstrates that the increase in cutting speed and depth of cut leads to the rise of R_a and θ. However, in the case of cutting speed, sudden blips are also noticeable for the output parameters. Conversely, when large values of cutting speed were used, the effect became important. Therefore, it can be concluded that cutting speed exhibited the maximum influence on the response variable (Table 5).

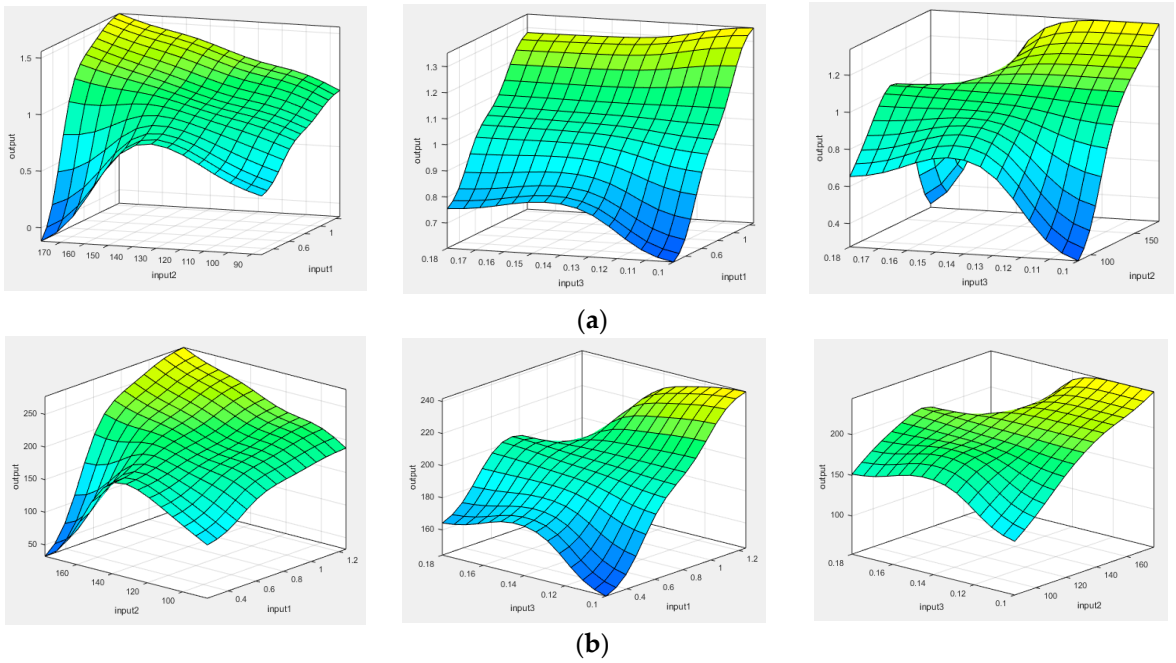

Figure 12. Variation of (**a**) surface roughness and (**b**) cutting temperature on different combinations of inputs (depth of cut, cutting speed, and feed rate).

4. Comparative Analysis

4.1. Comparison of Experimental Data with ANN and ANFIS Predicted Model

Mean absolute percentage error is used to measure the error of the process and was defined as Equation (1). *MAPE* calculation for the predicted values is shown in Table 11.

$$MAPE = \frac{APE}{Pj} \quad (1)$$

where $APE = \frac{tj-oj}{tj} \times 100$; t is the target value, o is the output value, and P is the number of samples.

The errors between the experimental and predicted values of R_a and θ are 3.95% and 3.45% when using a model based on ANN. Subsequently, the hybrid prediction model based on ANFIS was used to detect the deflection of the expected values from the experimental values to verify the percentage of process errors. MAPE was 1.072% and 1.172% for surface roughness and cutting temperature when predicting using the ANFIS model. It could be concluded that the hybrid method predicted the resulting output much more accurately since the amount of deviation was minimal compared to the predicted values of ANN. Nonetheless, ANN could also reasonably predict this value. Figures 13 and 14 show the disparity between the measured and predicted responses of R_a and F_z, which indicates the model's efficacy, as the predicted values for various combinations were closer to those of the experimentally reported readings.

4.2. Life Cycle Assessment and Sustainability Analysis

In the present research study, the empirical models for calculating production time, energy efficiency, specific cutting energy, and carbon emission were developed using a bottom-up approach, as presented in previous research [43]. Here, LCA and sustainability performance analysis, as per the design of the experiment, was presented in terms of production time, energy efficiency, specific cutting energy, and carbon emission. Figure 15 shows the LCA and sustainability performance outputs for dry and MQL-assisted machining of Al-based materials using the PCD tool.

Table 11. MAPE calculation using ANN- and ANFIS-based predictive models.

Run	Exp. Result		ANN Predicted Result		ANFIS Predicted Result	
	R_a	θ	R_a	θ	R_a	θ
	(μm)	(°C)	(μm)	(°C)	(μm)	(°C)
1	0.508	135.79	0.49	132.34	0.508	133
2	0.625	152.24	0.611	151.34	0.625	152
3	0.784	173.45	0.654	170.89	0.735	173
4	0.815	177.53	0.8	174.23	0.816	175
5	1.030	206.09	1.025	197.66	1.03	206
6	0.49	134.66	0.523	133.62	0.49	135
7	0.735	165.50	0.687	156.26	0.735	162
8	0.894	186.77	0.882	181.88	0.872	184
9	0.925	190.85	0.911	188.22	0.926	187
10	1.140	219.41	1.09	211.9	1.14	217
11	0.728	162.43	0.644	151.44	0.728	154
12	0.845	178.88	0.836	169.13	0.845	175
13	1.004	200.09	0.956	195.1	0.96	200
14	1.035	204.17	1.043	200.76	1.04	202
15	1.250	232.73	1.2	225.43	1.25	227
16	0.795	170.98	0.77	166.98	0.796	171
17	0.955	192.20	0.946	183.32	0.955	192
18	1.114	213.41	1.034	206.66	1.11	213
19	1.145	217.49	1.126	209	1.15	217
20	1.360	246.05	1.33	237.44	1.36	246
21	1.015	197.62	0.936	188.74	1.004	195
22	1.175	218.84	1.12	211.76	1.155	214
23	1.334	240.05	1.304	222.13	1.33	240
24	1.365	244.13	1.311	237.56	1.34	244
25	1.580	272.69	1.56	264	1.58	273
MAPE			3.95	3.45	1.072	1.172

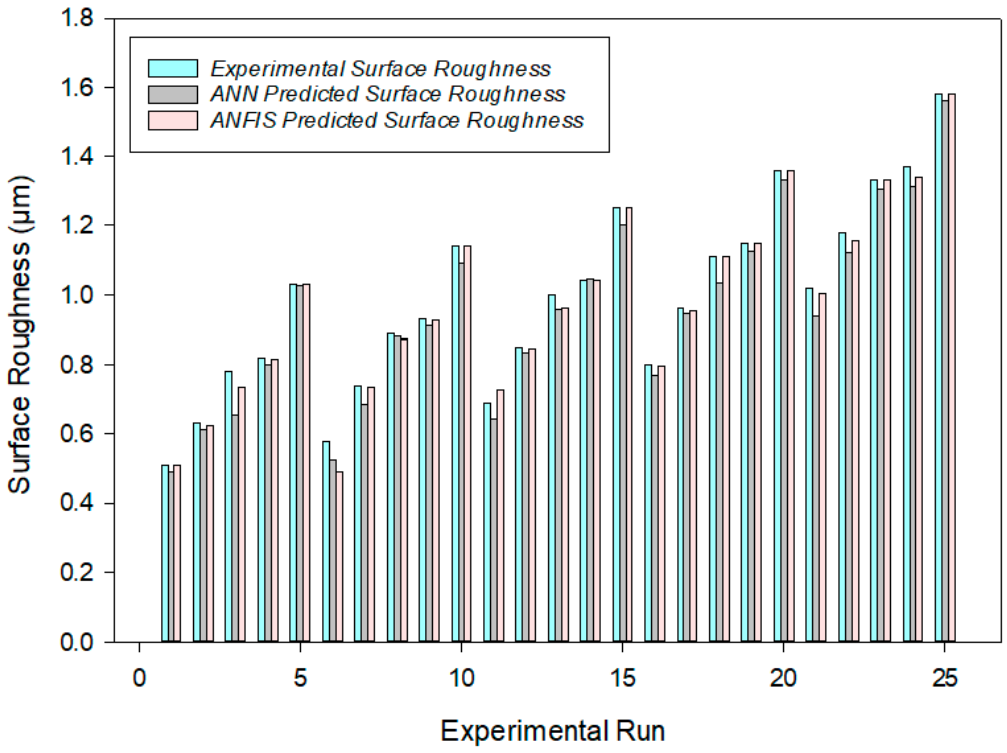

Figure 13. Comparison between experimental and predicted results of surface roughness.

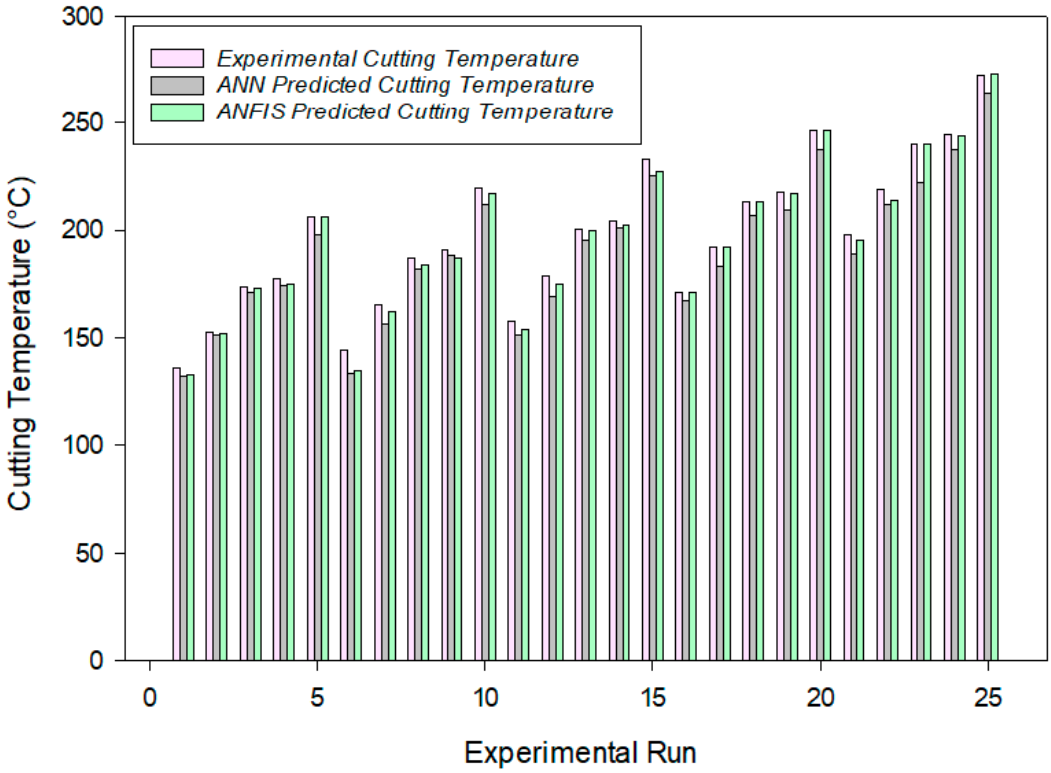

Figure 14. Comparison between experimental and predicted results of cutting temperature.

Every operation required a determined time to operate the machining process, called the "actual time" (Tam). Therefore, the total processing time included the idle time, air cutting time, cutting time, tool change time, and cooling/lubrication time, as calculated in Equations (2) and (3).

$$Processing\ time\ (T_c) = t_i + t_a + t_c + t_{tc} + t_{\frac{col}{lub}} \quad (2)$$

The idle time is the sum of stand-by time, material handling, and setup time.

$$Idle\ time\ (t_i) = t_{sb} + t_h + t_{su} \quad (3)$$

The total processing time for each experimental run after calculation is shown in Figure 15a. It can be seen that MQL-assisted machining takes less time for cutting job operation in comparison to dry-machining. The minimum process time was determined at the optimized setting and was 195 s. This was due to the tool having a longer tool life, which reduced the tool change time. In addition, the MQL cutting fluid helped to reduce the cutting temperature, dissipate heat from the machining zone, and improve the tool's efficiency and life. Similar observations have been made in previous research work [4,46].

The machining energy efficiency (η) was also considered an attribute for LCA and sustainability and is computed as shown in Equations (4)–(6).

$$Machining\ energy\ \text{efficiency}\ (\eta) = \frac{\text{Machining Energy}\ (E_m)}{Total\ Energy\ Consumed\ (E_T)} \quad (4)$$

where power consumption can be calculated by various stages of the machine tool, as shown in Equation (5).

$$Machine\ Power\ (P_m) = P_i t + P_a t + P_c t + P_{tc} t + P_{\frac{col}{lub}} t \quad (5)$$

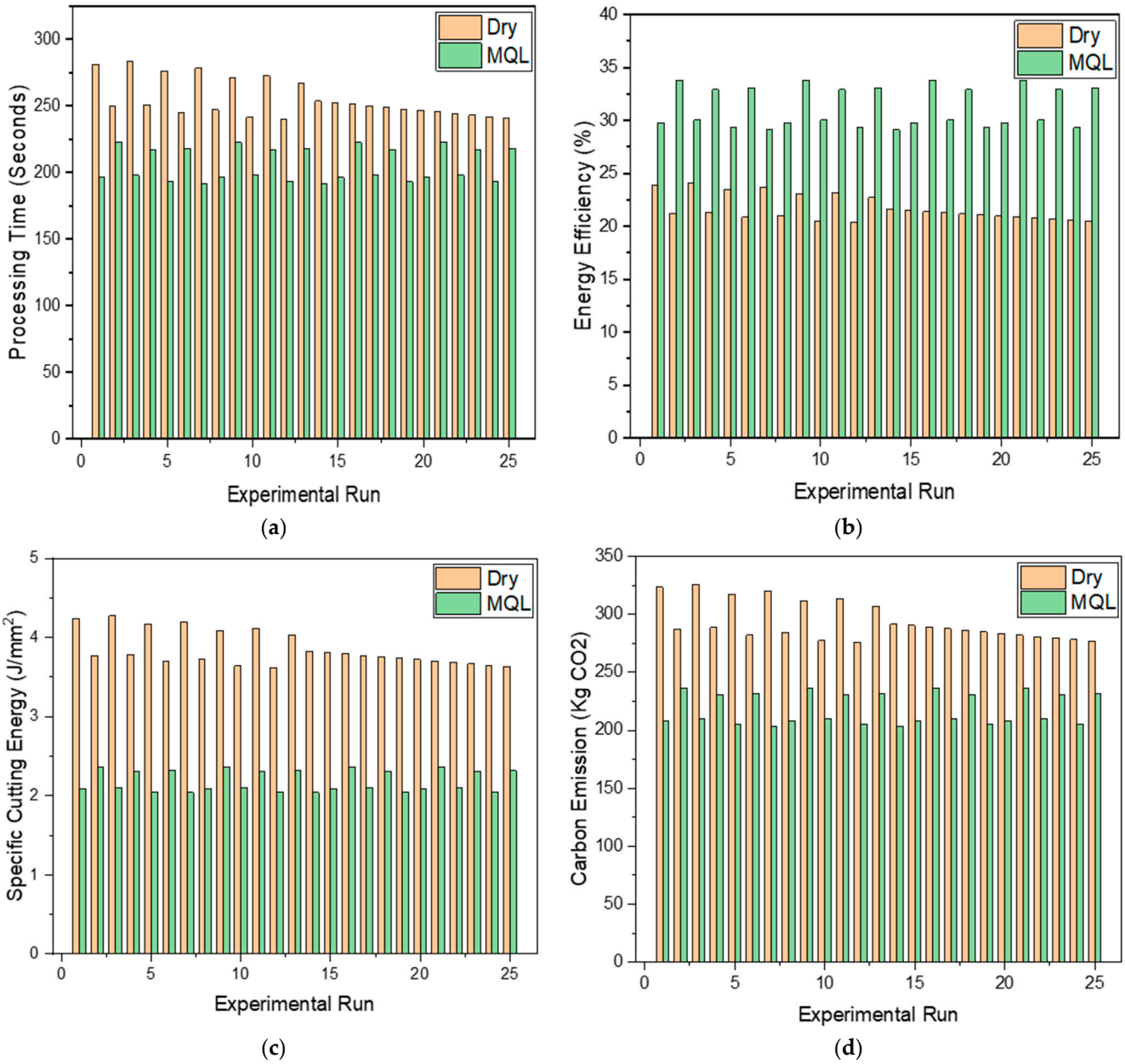

Figure 15. (**a**) Processing-time, (**b**) energy efficiency, (**c**) specific cutting energy, and (**d**) carbon emissions against the experimental run and cooling modes.

Energy consumption is expressed in Equation (6):

$$\text{Energy consumption} \quad (E_m) = \int_0^{t_i} P_i t dt + \int_0^{t_a} P_a t \, dt + \int_0^{t_c} P_c t dt + \int_0^{t_{tc}} P_{tc} t dt + \int_0^{t_{\frac{col}{lub}}} P_{\frac{col}{lub}} t dt \quad (6)$$

Figure 15b shows the machine energy efficiency in terms of the experimental run for dry and MQL-assisted machining. It can be seen that the machine energy efficiency varies in the range of 20–34%. Thus, the reduction in energy consumption and the reduction of waste energy in machine tools is not the only way to achieve a high energy efficiency. Thus, the primary objectives were to reduce energy consumption and waste generation. The results show that MQL-assisted machining has a high energy efficiency compared to dry

machining because the tool life is longer in MQL-assisted machining, which reduces tool change. This further reduced stand-by energy utilization in the tool changing phase.

Specific cutting energy (SCE) was also one of the key indicators of sustainability analysis. SCE is the ratio of total energy consumed to the material removal rate [47]. To reduce the SCE, either the material removal is increased using the same energy or a reduced energy consumption is needed for the same material removal, as presented in Equation (7).

$$SCE = \frac{E_m}{MRR} \tag{7}$$

Material removal rate (MRR) is calculated as per Equation (8).

$$MRR = V_c \times f \times a_p \tag{8}$$

Figure 15c shows the SCE concerning the experimental run for dry and MQL-assisted machining. It can be seen that the SCE varies in the range of 2–4 J/mm^2. From the results, it can be seen that MQL-assisted machining has a low SCE compared with dry-machining. The prime reason for this is dependent on the sharpness of the cutting edge of the tool. In the case of MQL-assisted machining, the tool cutting edge has a long-life cycle. Therefore, the tool's life depends on its cutting edge sharpness, which requires a low cutting force and energy to perform job operations. Moreover, there is no built-up-edge formation in the process, which increases the tool life and maintains the cutting edge's sharpness because MQL-lubrication disposes of the heat energy generated in the machining zone. As a result, the long-life sharp edge produced a high material removal, and less tool change, which reduced cutting power consumption, which reduced the SCE.

Carbon emissions (CO_2) can be termed as another significant indicator of sustainability. The energy consumption indirectly calculates carbon emissions via machine tools. The total carbon emission (CE_{total}) is calculated as per Equation (9).

$$CE_p = CES \times (E_i + E_a + E_c + E_{tc} + E_l) + CF_{CT} \times \frac{t_c}{T_L} + CF_{MQL} \times Q_{MQL} \times t_c \tag{9}$$

Figure 15d shows the variations in CO_2 concerning experimental run for dry and MQL-assisted machining. The carbon emissions under the obtained sustainable machining process were in the range of 200 to 300 kg-CO_2. However, it can be seen that the CO_2 emissions were comparatively much lower in MQL-assisted machining as compared to dry machining. This is because, in MQL machining, a very nominal amount of cutting fluid is used, which generates a smaller carbon footprint. Moreover, less energy consumption is required in MQL machining to achieve high degree of material removal and a very low tool change. In this, savings in energy, time, money, as well as for the environment occur, making MQL a sustainable machining process [43,48–50].

The obtained results are in line with previously published research work. Khan et al. reported investigating Al2O3-based nano-fluid-assisted MQL machining in terms of technological and economic factors [51]. Various sustainable parameters, such as energy, cost, and carbon emission were studied. It has been reported that nano-fluid-assisted MQL machining reduces the cost per unit of the product and achieves a low carbon manufacturing goal [52]. Gupta et al. studied the environmental and sustainability aspects of hybrid-cooling-assisted machining of Ti-6Al-4 V alloy [53]. It was reported that LN_2 and MQL were the most effective cooling systems and helped in reducing the production time, energy, cost, and carbon emissions. Similar to the above-mentioned studies, the current study also presented that MQL machining reduces production time, energy, cost, and carbon emissions while processing Al-based alloys. Other sustainability indices, such as human wellbeing, pollution, vibrations, etc., will be considered in future research.

5. Conclusions

Current research focuses on the sustainability aspect of machining Al-based alloy using the PCD tool. At the same time, various machining attributes (surface roughness and cutting temperature) were also addressed to interrelate the effect of input parameters on the resultant responses. The addition of Zr in the material preparation significantly impacted reducing the cutting temperature under MQL cutting conditions. Based on the research, the following conclusions can be made.

From ANOVA analyses, it is understandable that the cutting velocity was the most dominant factor, followed by the depth of cut, to induce a preferable value for both the response parameters, which was also aligned with the SN ratio results attainted. As such, both methods can give assurances regarding the identification of the dominant factors affecting the response variables.

The SN ratio response graph demonstrates that, to obtain the optimum surface roughness and cutting temperature, a combination of parameters with a depth of cut of 0.25 mm, cutting speed of 86 m/min, and feed rate of 0.10 mm/rev was desirable. On the other hand, DFA showed the optimum surface roughness and cutting temperature, with a combination of 0.305 mm for the depth of cut, 86 m/min for cutting speed, and a 0.10 mm/rev for feed rate. Moreover, the highest perceived value of 0.997 could be attained amongst the 92 solutions while setting the mentioned parameters.

The ANN-based model effectively established a link between the input factors and response variables for the testing dataset and the training dataset. It could also be observed that the mean absolute percentage error fell to a good range of values of 3.25% to 3.95% for the response variables. The deviation chart indicated the acceptability of the Sugeno hybrid ANFIS prediction model, with mean absolute percentage errors of 1.071% and 1.72%, respectively, for surface roughness and cutting temperature, demonstrating the capacity to predict the performance of the responses more reliably than the ANN model.

MQL-assisted machining has been proven to be a sustainable machining process as compared to dry-machining. In MQL machining, owing to the very nominal use of cutting fluid, it generates a smaller carbon footprint. Moreover, significantly less energy consumption is required in MQL machining to achieve a high material removal and very low tool changes were needed. In this, there are savings in terms of energy, time, money, and the environment, making MQL a sustainable machining process.

It appears that the minimum quantity of lubrication could play a prominent role in maintaining the sustainability aspect of machining of the chosen material. Nevertheless, before applying this method for frequent industrial applications, more research needs to be done on the machining behavior considering higher cutting speeds and various nose radii of the PCD tool.

A limitation of current research work is that other sustainability indexes, such as human wellbeing, pollution, vibrations, etc., are not covered and will be considered in future research work.

Author Contributions: Data curation, M.R.K., C.P. and C.I.P.; Formal analysis, J.B.T., S.M.M. and R.K.; Investigation, A.H., S.S., R.K. and Y.N.; Resources, S.H.S.; Software, R.K. and Y.N.; Supervision, Y.N.; Validation, Y.N.; Writing—original draft, C.I.P. All authors have read and agreed to the published version of the manuscript.

Funding: This research received no external funding.

Institutional Review Board Statement: Not applicable.

Informed Consent Statement: Not applicable.

Data Availability Statement: Not applicable.

Acknowledgments: The authors would like to express their gratitude towards the Department of Mechanical and Production Engineering, AUST, for allowing us to conduct the research work using their laboratory facilities.

Conflicts of Interest: The authors declare no conflict of interest.

References

1. Ezugwu, E.O. Improvements in the machining of aero-engine alloys using self-propelled rotary tooling technique. *J. Mater. Process. Technol.* **2007**, *185*, 60–71. [CrossRef]
2. Verma, R.; Ghosh, A.K.; Kim, S.; Kim, C. Grain refinement and superplasticity in 5083 Al. *Mater. Sci.Eng. A* **1995**, *191*, 143–150. [CrossRef]
3. Heath, P.J. Developments in applications of PCD tooling. *J. Mater. Process. Technol.* **2001**, *116*, 31–38. [CrossRef]
4. Maeng, D.Y.; Lee, J.H.; Hong, S.I. The effect of transition elements on the superplastic behavior of Al–Mg alloys. *Mater. Sci. Eng. A* **2003**, *357*, 188–195. [CrossRef]
5. Sarıkaya, M.; Güllü, A. Multi-response optimization of minimum quantity lubrication parameters using Taguchi-based grey relational analysis in turning of difficult-to-cut alloy Haynes 25. *J. Clean. Prod.* **2015**, *91*, 347–357. [CrossRef]
6. Dhar, N.R.; Kamruzzaman, M. Cutting temperature, tool wear, surface roughness and dimensional deviation in turning AISI-4037 steel under cryogenic condition. *Int. J. Mach. Tools Manuf.* **2007**, *47*, 754–759. [CrossRef]
7. Krolczyk, G.M.; Maruda, R.W.; Krolczyk, J.B.; Wojciechowski, S.; Mia, M.; Nieslony, P.; Budzik, G. Ecological trends in machining as a key factor in sustainable production—A review. *J. Clean. Prod.* **2019**, *218*, 601–615. [CrossRef]
8. Sreejith, P.S.; Krishnamurthy, R.; Malhotra, S.K.; Narayanasamy, K. Evaluation of PCD tool performance during machining of carbon/phenolic ablative composites. *J. Mater. Process. Technol.* **2000**, *104*, 53–58. [CrossRef]
9. Alagan, N.T.; Beno, T.; Wretland, A. Investigation of Modified Cutting Insert with Forced Coolant Application in Machining of Alloy 718. *Procedia CIRP* **2016**, *42*, 481–486. [CrossRef]
10. Teti, R. Machining of Composite Materials. *CIRP Ann.* **2002**, *51*, 611–634. [CrossRef]
11. Brun, M.K.; Lee, M.; Gorsler, F. Wear characteristics of various hard materials for machining sic-reinforced aluminum alloy. *Wear* **1985**, *104*, 21–29. [CrossRef]
12. Weinert, K.; König, W. A Consideration of Tool Wear Mechanism when Machining Metal Matrix Composites (MMC). *CIRP Ann.* **1993**, *42*, 95–98. [CrossRef]
13. Andrewes, C.J.E.; Feng, H.-Y.; Lau, W.M. Machining of an aluminum/SiC composite using diamond inserts. *J. Mater. Process. Technol.* **2000**, *102*, 25–29. [CrossRef]
14. Dhar, N.R.; Kamruzzaman, M.; Ahmed, M. Effect of minimum quantity lubrication (MQL) on tool wear and surface roughness in turning AISI-4340 steel. *J. Mater. Process. Technol.* **2006**, *172*, 299–304. [CrossRef]
15. Sivaiah, P.; Chakradhar, D. The Effectiveness of a Novel Cryogenic Cooling Approach on Turning Performance Characteristics During Machining of 17-4 PH Stainless Steel Material. *Silicon* **2019**, *11*, 25–38. [CrossRef]
16. Kaynak, Y.; Gharibi, A. Progressive Tool Wear in Cryogenic Machining: The Effect of Liquid Nitrogen and Carbon Dioxide. *J. Manuf. Mater. Process.* **2018**, *2*, 31. [CrossRef]
17. Rabiei, F.; Rahimi, A.R.; Hadad, M.J.; Ashrafijou, M. Performance improvement of minimum quantity lubrication (MQL) technique in surface grinding by modeling and optimization. *J. Clean. Prod.* **2015**, *86*, 447–460. [CrossRef]
18. Park, K.-H.; Ewald, B.; Kwon, P.Y. Effect of Nano-Enhanced Lubricant in Minimum Quantity Lubrication Balling Milling. *J. Tribol.* **2011**, *133*. [CrossRef]
19. Alok, A.; Das, M. Multi-objective optimization of cutting parameters during sustainable dry hard turning of AISI 52100 steel with newly develop HSN2-coated carbide insert. *Measurement* **2019**, *133*, 288–302. [CrossRef]
20. Shihab, S.K.; Khan, Z.A.; Mohammad, A.; Siddiqueed, A.N. RSM based study of cutting temperature during hard turning with multilayer coated carbide insert. *Procedia Mater. Sci.* **2014**, *6*, 1233–1242. [CrossRef]
21. Shastri, A.; Nargundkar, A.; Kulkarni, A.J.; Benedicenti, L. Optimization of process parameters for turning of titanium alloy (Grade II) in MQL environment using multi-CI algorithm. *SN Appl. Sci.* **2021**, *3*, 226. [CrossRef]
22. Karim, M.R.; Shawon, S.H.; Morshed, S.M.; Hasan, A.; Tariq, J.B. *Investigation of Surface Roughness in MQL Aided Turning of Al/Cu/Zr Alloy Using PCD Tool*; Springer: Singapore, 2020; p. 207.
23. Karim, M.R.; Siddique, R.A.; Dilwar, F. Study of Surface Roughness and MRR in Turning of SiC Reinforced Al Alloy Composite Using Taguchi Design Method, ANN and PCA Approach under MQL Cutting Condition. *Adv. Mater. Res.* **2020**, *1158*, 115–131. [CrossRef]
24. Hadad, M.; Sadeghi, B. Minimum quantity lubrication-MQL turning of AISI 4140 steel alloy. *J. Clean. Prod.* **2013**, *54*, 332–343. [CrossRef]
25. Thakur, A.; Manna, A.; Samir, S. Multi-Response Optimization of Turning Parameters during Machining of EN-24 Steel with SiC Nanofluids Based Minimum Quantity Lubrication. *Silicon* **2020**, *12*, 71–85. [CrossRef]
26. Lin, C.L. Use of the Taguchi Method and Grey Relational Analysis to Optimize Turning Operations with Multiple Performance Characteristics. *Mater. Manuf. Process.* **2004**, *19*, 209–220. [CrossRef]
27. Varol, T.; Canakci, A.; Ozsahin, S. Artificial neural network modeling to effect of reinforcement properties on the physical and mechanical properties of Al2024–B4C composites produced by powder metallurgy. *Compos. Part B Eng.* **2013**, *54*, 224–233. [CrossRef]
28. Bachy, B.; Franke, J. Modeling and optimization of laser direct structuring process using artificial neural network and response surface methodology. *Int. J. Ind. Eng. Comput.* **2015**, *6*, 553–564. [CrossRef]

29. Das, B.; Roy, S.; Rai, R.N.; Saha, S.C. Studies on Effect of Cutting Parameters on Surface Roughness of Al-Cu-TiC MMCs: An Artificial Neural Network Approach. *Procedia Comput. Sci.* **2015**, *45*, 745–752. [CrossRef]
30. Davim, J.P.; Gaitonde, V.N.; Karnik, S.R. Investigations into the effect of cutting conditions on surface roughness in turning of free machining steel by ANN models. *J. Mater. Process. Technol.* **2008**, *205*, 16–23. [CrossRef]
31. Pandiyan, V.; Caesarendra, W.; Tjahjowidodo, T.; Praveen, G. Predictive Modelling and Analysis of Process Parameters on Material Removal Characteristics in Abrasive Belt Grinding Process. *Appl. Sci.* **2017**, *7*, 363. [CrossRef]
32. Reddy, B.S.; Kumar, J.S.; Reddy, K.V.K. Prediction of surface roughness in turning using adaptive neuro-fuzzy inference system. *Jordan J. Mech. Ind. Eng.* **2009**, *3*, 252–259.
33. Karim, M.; Dilwar, F.; Siddique, R. Predictive Modeling of Surface Roughness in MQL assisted Turning of SiC-Al Alloy Composites using Artificial Neural Network and Adaptive Neuro Fuzzy Inference System. *J. Adv. Res. Manuf. Mater. Sci. Metall. Eng.* **2019**, *5*, 12–28.
34. Kumar, R.; Bilga, P.S.; Singh, S. An Investigation of Energy Efficiency in Finish Turning of EN 353 Alloy Steel. *Procedia CIRP* **2021**, *98*, 654–659. [CrossRef]
35. Kumar, R.; Singh, S.; Bilga, P.S.; Jatin, K.; Singh, J.; Singh, S.; Scutaru, M.-L.; Pruncu, C.I. Revealing the benefits of entropy weights method for multi-objective optimization in machining operations: A critical review. *J. Mater. Res. Technol.* **2021**, *10*, 1471–1492. [CrossRef]
36. Kishawy, H.A.; Hegab, H.; Deiab, I.; Eltaggaz, A. Sustainability Assessment during Machining Ti-6Al-4V with Nano-Additives-Based Minimum Quantity Lubrication. *J. Manuf. Mater. Process.* **2019**, *3*, 61. [CrossRef]
37. Liu, Z.Y.; Li, C.; Fang, X.Y.; Guo, Y.B. Cumulative energy demand and environmental impact in sustainable machining of inconel superalloy. *J. Clean. Prod.* **2018**, *181*, 329–336. [CrossRef]
38. Frischknecht, R.; Wyss, F.; Knöpfel, S.B.; Lützkendorf, T.; Balouktsi, M. Cumulative energy demand in LCA: The energy harvested approach. *Int. J. Life Cycle Assess.* **2015**, *20*, 957–969. [CrossRef]
39. Ic, Y.T.; Güler, E.S.; Cabbaroğlu, C.; Yüksel, E.D.; Sağlam, H.M. Optimisation of cutting parameters for minimizing carbon emission and maximising cutting quality in turning process. *Int. J. Prod. Res.* **2018**, *56*, 4035–4055. [CrossRef]
40. Branker, K.; Adams, D.; Jeswiet, J. Initial analysis of cost, energy and carbon dioxide emissions in single point incremental forming—Producing an aluminium hat. *Int. J. Sustain. Eng.* **2012**, *5*, 188–198. [CrossRef]
41. Jamil, M.; Khan, A.M.; He, N.; Li, L.; Iqbal, A.; Mia, M. Evaluation of machinability and economic performance in cryogenic-assisted hard turning of α-β titanium: A step towards sustainable manufacturing. *Mach. Sci. Technol.* **2019**, *23*, 1022–1046. [CrossRef]
42. Santos, M.C.; Machado, A.R.; Barrozo, M.A. Temperature in machining of aluminum alloys. In *Temperature Sensing*; Books on Demand: Norderstedt, Germany, 2018; p. 71. [CrossRef]
43. Bilga, P.S.; Singh, S.; Kumar, R. Optimization of energy consumption response parameters for turning operation using Taguchi method. *J. Clean. Prod.* **2016**, *137*, 1406–1417. [CrossRef]
44. Padilla-Atondo, J.M.; Limon-Romero, J.; Perez-Sanchez, A.; Tlapa, D.; Baez-Lopez, Y.; Puente, C.; Ontiveros, S. The Impact of Hydrogen on a Stationary Gasoline-Based Engine through Multi-Response Optimization: A Desirability Function Approach. *Sustainability* **2021**, *13*, 1385. [CrossRef]
45. Jeswiet, J.; Kara, S. Carbon emissions and CES™ in manufacturing. *CIRP Ann.* **2008**, *57*, 17–20. [CrossRef]
46. Khan, A.M.; Anwar, S.; Jamil, M.; Nasr, M.M.; Gupta, M.K.; Saleh, M.; Ahmad, S.; Mia, M. Energy, Environmental, Economic, and Technological Analysis of Al-GnP Nanofluid- and Cryogenic LN2-Assisted Sustainable Machining of Ti-6Al-4V Alloy. *Metals* **2021**, *11*, 88. [CrossRef]
47. Kumar, R.; Singh, S.; Sidhu, A.S.; Pruncu, C.I. Bibliometric Analysis of Specific Energy Consumption (SEC) in Machining Operations: A Sustainable Response. *Sustainability* **2021**, *13*, 5617. [CrossRef]
48. Kumar, R.; Bilga, P.S.; Singh, S. Optimization of Active Cutting Power Consumption by Taguchi Method for Rough Turning of Alloy Steel. *Int. J. Metall. Alloys* **2020**, *6*, 37–45. Available online: http://materials.journalspub.info/index.php?journal=IJM&page=article&op=view&path%5B%5D=632 (accessed on 1 December 2020).
49. Kumar, R.; Bilga, P.S.; Singh, S. Optimization and Modeling of Active Power Consumption for Turning Operations. In Proceedings of the ISME 19th Conference on Advances in Mechanical Engineering (Mechanical Systems and Sustainability), Jalandhar, Punjab, India, 20–22 December 2018; Dr. B. R. Ambedkar National Institute of Technology Jalandhar: Punjab, India; pp. 1–16.
50. Kumar, R.; Bilga, P.S.; Singh, S. Multi objective optimization using different methods of assigning weights to energy consumption responses, surface roughness and material removal rate during rough turning operation. *J. Clean. Prod.* **2017**, *164*, 45–57. [CrossRef]
51. Khan, A.M.; Liang, L.; Mia, M.; Gupta, M.K.; Wei, Z.; Jamil, M.; Ning, H. Development of process performance simulator (PPS) and parametric optimization for sustainable machining considering carbon emission, cost and energy aspects. *Renew. Sustain. Energy Rev.* **2021**, *139*, 110738. [CrossRef]
52. Chandel, R.S.; Kumar, R.; Kapoor, J. Sustainability aspects of machining operations: A summary of concepts. *Mater. Today Proc.* **2021**. [CrossRef]
53. Gupta, M.K.; Song, Q.; Liu, Z.; Sarikaya, M.; Jamil, M.; Mia, M.; Kushvaha, V.; Singla, A.K.; Li, Z. Ecological, economical and technological perspectives based sustainability assessment in hybrid-cooling assisted machining of Ti-6Al-4 V alloy. *Sustain. Mater. Technol.* **2020**, *26*, e00218. [CrossRef]